Cell

Transcriptional Repression of PGC-1α by Mutant Huntingtin Leads to Mitochondrial Dysfunction and Neurodegeneration

Libin Cui,[1] Hyunkyung Jeong,[1] Fran Borovecki,[1] Christopher N. Parkhurst,[2] Naoko Tanese,[2] and Dimitri Krainc[1,*]
[1] Department of Neurology, Massachusetts General Hospital, Harvard Medical School, MassGeneral Institute for Neurodegeneration, Charlestown, MA 02129 USA
[2] Department of Microbiology, New York University School of Medicine, New York, NY 10016 USA
*Contact: krainc@helix.mgh.harvard.edu
DOI 10.1016/j.cell.2006.09.015

SUMMARY

Huntington's disease (HD) is an inherited neurodegenerative disease caused by a glutamine repeat expansion in huntingtin protein. Transcriptional deregulation and altered energy metabolism have been implicated in HD pathogenesis. We report here that mutant huntingtin causes disruption of mitochondrial function by inhibiting expression of PGC-1α, a transcriptional coactivator that regulates several metabolic processes, including mitochondrial biogenesis and respiration. Mutant huntingtin represses PGC-1α gene transcription by associating with the promoter and interfering with the CREB/TAF4-dependent transcriptional pathway critical for the regulation of PGC-1α gene expression. Crossbreeding of PGC-1α knockout (KO) mice with HD knockin (KI) mice leads to increased neurodegeneration of striatal neurons and motor abnormalities in the HD mice. Importantly, expression of PGC-1α partially reverses the toxic effects of mutant huntingtin in cultured striatal neurons. Moreover, lentiviral-mediated delivery of PGC-1α in the striatum provides neuroprotection in the transgenic HD mice. These studies suggest a key role for PGC-1α in the control of energy metabolism in the early stages of HD pathogenesis.

INTRODUCTION

Huntington's disease (HD) is a progressive and fatal neurological disorder that is characterized phenotypically by involuntary movements and psychiatric disturbances (Vonsattel and DiFiglia, 1998). The gene huntingtin, which is mutated in HD patients, contains an expanded polyglutamine repeat within exon 1. The number of polyglutamine diseases continues to grow, and they share several common features, including neurodegeneration, a dominant pattern of inheritance and genetic anticipation (Zoghbi and Orr, 2000). In HD, mutant huntingtin is expressed ubiquitously, but selective cell loss is observed in the brain, particularly in the caudate and putamen of the striatum (Vonsattel and DiFiglia, 1998).

Many proteins containing polyglutamine-rich regions function as transcription factors (Alba and Guigo, 2004). Interactions of mutant huntingtin with several transcription factors have been demonstrated, suggesting that mutant huntingtin may be directly involved in the regulation of gene transcription (Sugars and Rubinsztein, 2003). For example, mutant huntingtin was shown to repress transcription by interfering with activator/coactivator interactions (Sp1/TAF4) in brain samples from presymptomatic patients (Dunah et al., 2002). These studies suggested that a soluble form of mutant huntingtin may interfere with specific components of transcriptional machinery in early stages of HD.

In addition to transcriptional deregulation, altered energy metabolism has been implicated in HD pathogenesis (Browne and Beal, 2004). Striatal hypometabolism was detected in asymptomatic HD subjects, and activities of complexes of the electron transport chain were selectively reduced in caudate and putamen of advanced-grade HD patients (Antonini et al., 1996; Grafton et al., 1992; Kuwert et al., 1993; Browne and Beal, 2004). Additional evidence that energetic deficits may contribute to neurodegeneration in HD came from studies showing that agents that enhance energy production in the brain were neuroprotective (Browne and Beal, 2004). However, the mechanism by which mutant huntingtin disrupts mitochondrial function and oxidative metabolism remains unclear.

In this study we demonstrate that mutant huntingtin interferes with energy metabolism by transcriptional repression of PGC-1α (peroxisome proliferator-activated receptor gamma coactivator-1 α). PGC-1α is a transcriptional coactivator that regulates several metabolic processes, including mitochondrial biogenesis and oxidative phosphorylation (Puigserver and Spiegelman, 2003; Finck

and Kelly, 2006). We show that PGC-1α plays an important role in brain energy homeostasis and represents a key target of mutant huntingtin in the pathogenesis of HD.

RESULTS

Decreased Expression of PGC-1α in Striatum of HD Brain

Recent findings suggest that striatum, the region most affected in HD, may be particularly susceptible to disruption of energy metabolism caused by lack of PGC-1α (Lin et al., 2004; Leone et al., 2005). To determine whether PGC-1α expression may be altered in the striatum, we examined PGC-1α mRNA in postmortem brain samples from presymptomatic HD patients. We found a 30% decrease of PGC-1α mRNA in the caudate nucleus of striatum, whereas no significant changes in PGC-1α expression were detected in the hippocampus or cerebellum in these brain samples (Figure 1A). These results indicate that PGC-1α expression is specifically decreased in the caudate, the first region affected in HD.

To examine whether PGC-1α downregulation leads to alterations in the expression of genes involved in energy metabolism, we first analyzed mRNA expression in the striatum of PGC-1α knockout (KO) mice by microarrays. Using gene-set enrichment analysis (GSEA), we found that metabolic pathways involved in mitochondrial function were among the most significantly decreased in PGC-1α KO striata (Figure S1A) (Subramanian et al., 2005). Comparisons of pathways significantly downregulated in PGC-1α KO mice with those downregulated in striata from early-stage human HD revealed several common pathways involving oxidative phosphorylation, mitochondrion, and the electron transport chain (Figure 1B) (Hodges et al., 2006). Decreased expression of a subset of mitochondrial genes in human HD brain was confirmed by real-time PCR (Figure S1B). These findings suggest that reduced expression of PGC-1α and its mitochondrial targets may represent an early dysfunction in HD pathogenesis.

The striatum comprises approximately 90% medium spiny projection neurons (MSN) and 10% aspiny interneurons. In HD, medium spiny neurons degenerate whereas striatal interneurons are spared, but the molecular mechanism of this preferential neuronal vulnerability is unknown (Ferrante et al., 1985). Since we find that the levels of PGC-1α are decreased in HD striatum, we used laser capture microdissection (LCM) and quantitative real-time PCR to analyze the expression of PGC-1α in individual striatal MSN or nNOS interneurons. When compared with normal mice, PGC-1α levels were decreased 5.6-fold in MSN isolated from HD knockin (KI) mice (Menalled et al. 2003) (Figure 1C). In contrast, PGC-1α was increased by 47-fold in HD interneurons, as compared with normal striatal interneurons (Figure 1D). These results suggest that decreased expression of PGC-1α may contribute to increased vulnerability of MSN observed in HD, whereas nNOS interneurons may be protected by high levels of PGC-1α.

To further examine the function of PGC-1α in the context of HD, we next analyzed levels of PGC-1α in a well-established model of striatal neuronal cell lines generated from HD KI mice (Trettel et al., 2000). These cell lines (*STHdh*^{Q111}) express endogenous mutant huntingtin and display mutant phenotype, including decreased cAMP synthesis and reduced ATP levels consistent with altered energy metabolism (Gines et al., 2003). We compared expression of PGC-1α and its mitochondrial targets in wild-type *STHdh*^{Q7} and mutant *STHdh*^{Q111} cells and found that expression of both PGC-1α and mitochondrial genes such as cytochrome C and COXIV were significantly decreased in *STHdh*^{Q111} cells (Figures 1E and 1F). PGC-1α mRNA level was reduced approximately 10-fold in mutant cells compared to the wild-type control. These results suggest that decreased levels of PGC-1α might play a role in mediating energy defects in mutant *STHdh*^{Q111} striatal cells.

Mutant Huntingtin Inhibits CRE-Dependent Transcription of PGC-1α Promoter

Recent findings suggest that mutant huntingtin may be involved in the regulation of gene transcription as a co-repressor (Dunah et al., 2002; Zhai et al., 2005; Sugars and Rubinsztein, 2003). To elucidate the mechanisms of PGC-1α downregulation observed in HD brain and *STHdh*^{Q111} cells, we next investigated whether mutant huntingtin may repress the PGC-1α promoter. The PGC-1α promoter reporter, encompassing −2533 to +78 of the mouse PGC-1α gene, was transfected into striatal cell lines from the wild-type and HD mutant mice. A dramatic inhibition of the reporter was observed in the mutant cells (*STHdh*^{Q111}) compared to the wild-type cells (*STHdh*^{Q7}) (Figure 2A). In order to examine whether mutant huntingtin directly inhibits the reporter, wild-type cells (*STHdh*^{Q7}) were transfected with increasing concentrations of normal and mutant huntingtin along with the PGC-1α reporter. Transfected mutant huntingtin significantly repressed the PGC-1α reporter in a dose-dependent manner (Figure 2B), suggesting that mutant huntingtin modulates the expression of the PGC-1α gene at the level of transcription.

Since *STHdh*^{Q111} cells exhibit decreased cAMP levels (Gines et al., 2003), we next investigated whether treatment of these cells with cAMP could affect the PGC-1α reporter activity. As shown in Figure 2C, treatment of *STHdh*^{Q111} mutant cells with 8-bromo-cAMP was able to significantly upregulate the activity of the PGC-1α reporter. Importantly, these effects were dependent on the CRE binding site in the PGC-1α proximal promoter, which is known to be critically important for PGC-1α regulation in several tissues (Herzig et al. 2001). The reduced expression of PGC-1α mRNA in *STHdh*^{Q111} cells and upregulation of the PGC-1α reporter by cAMP prompted us to examine whether endogenous PGC-1α mRNA was modulated by cAMP in *STHdh*^{Q111} cells. Treatment of these cells with cAMP significantly upregulated PGC-1α mRNA levels (Figure 2D). Taken together, these results suggest

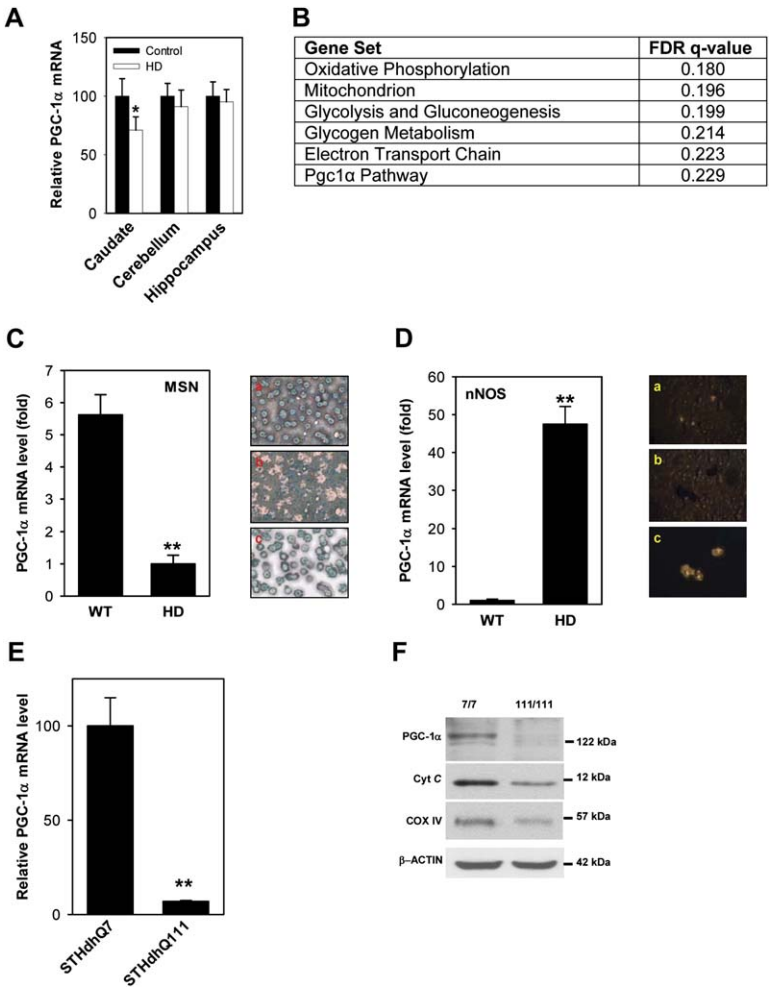

Gene Set	FDR q-value
Oxidative Phosphorylation	0.180
Mitochondrion	0.196
Glycolysis and Gluconeogenesis	0.199
Glycogen Metabolism	0.214
Electron Transport Chain	0.223
Pgc1α Pathway	0.229

Figure 1. Decreased Levels of PGC-1α mRNA in Human and Mouse HD Brain

(A) Total RNA was isolated from the caudate nucleus, cerebellum, and hippocampus of the postmortem brain tissues of presymptomatic HD subjects and normal controls. Samples were analyzed by quantitative real-time PCR with gene-specific primers and normalized to 28S RNA. Graphs represent means ± SEM of three independent experiments. *$p < 0.01$ versus control.

(B) Gene-set enrichment analysis reveals overlapping gene sets that are significantly decreased in striata of PGC-1α KO mice and HD patients. Data sets with false discovery rate (FDR) Q value ≤ 0.25 are presented.

(C) PGC-1α mRNA is decreased in KI HD mice (HD) medium spiny neurons (MSN) compared to wild-type (WT) mice MSN. Left panel shows Q-PCR analysis of PGC-1α mRNA in laser capture microdissected (LCM) MSN from 12-month-old KI ($n = 4$) and wild-type mice ($n = 4$). The bars represent means ± SEM fold change normalized to control, **$p < 0.0001$ versus wild-type. Right panel shows methylene blue-stained MSN before (a) and after dissection (b) and dissected MSN neurons attached to a thermoplastic film (c).

(D) PGC-1α mRNA is increased in HD KI mice nNOS interneurons compared to wild-type nNOS interneurons. Analysis was performed as in (C). The bars represent means ± SEM fold change normalized to control, **$p < 0.0001$ versus wild-type.

(E) PGC-1α mRNA is decreased in mutant $STHdh^{Q111}$ striatal cell line. mRNA levels of PGC-1α in wild-type $STHdh^{Q7}$ and mutant $STHdh^{Q111}$ striatal cell lines were measured by quantitative real-time PCR and normalized to β-actin mRNA. Expression levels of endogenous normal and mutant huntingtin were comparable as verified by Western blotting (not shown). Graphs represent means ± SEM of three independent experiments. *$p < 0.0001$ versus control.

(F) PGC-1α and mitochondrial protein levels are decreased in mutant striatal cell lines. Western blotting was performed using 40 μg of total cell extracts from $STHdh^{Q7}$ and $STHdh^{Q111}$ cell lines expressing endogenous normal (Q7/7) and mutant (Q111/111) huntingtin, respectively. Antibodies specific for PGC-1α, cytochrome C oxidase complex IV subunit I (COX IV) and cytochrome C were used. β-actin was used as loading control. Experiments were done in triplicate.

that PGC-1α gene repression by mutant huntingtin involves CRE-dependent transcription.

To examine the mechanism of regulation of the PGC-1α promoter by mutant huntingtin in relevant target cells, primary striatal neurons were transfected with PGC-1α promoter reporter along with mutant or normal huntingtin. Although huntingtin with normal glutamine repeats (HttQ17) had no significant effect on the promoter activity, mutant huntingtin (HttQ75) produced significant inhibition by more than 75% compared to the normal huntingtin (Figure 2E). To determine whether the inhibition of CRE-mediated transcription was dependent on increased levels of huntingtin relative to those of endogenous CREB, we overexpressed CREB together with huntingtin. We found that overexpression of CREB that is constitutively active (Du et al., 2000) significantly reduced but did not rescue the inhibitory effects of mutant huntingtin on PGC-1α promoter reporter (Figure 2E). These effects of CREB were dependent on the CRE site on the PGC-1α promoter, because no significant effect was seen when the CRE site was mutated (not shown).

We have previously shown that huntingtin interacts with TAF4 at least in part in the context of TFIID complex and that TAF4 plays a critical role in mediating mutant huntingtin effects on Sp1-driven gene transcription (Dunah et al., 2002). In addition to its function in Sp1 transcription, TAF4 also mediates coupling of CREB to TFIID and the basal transcriptional machinery (Saluja et al., 1998; Shimohata et al., 2000). Therefore, we examined whether CREB/TAF4 is required for maximal activity of the PGC-1α promoter. As shown in Figure 2E, coexpression of TAF4 and CREB resulted in complete reversal of huntingtin-induced

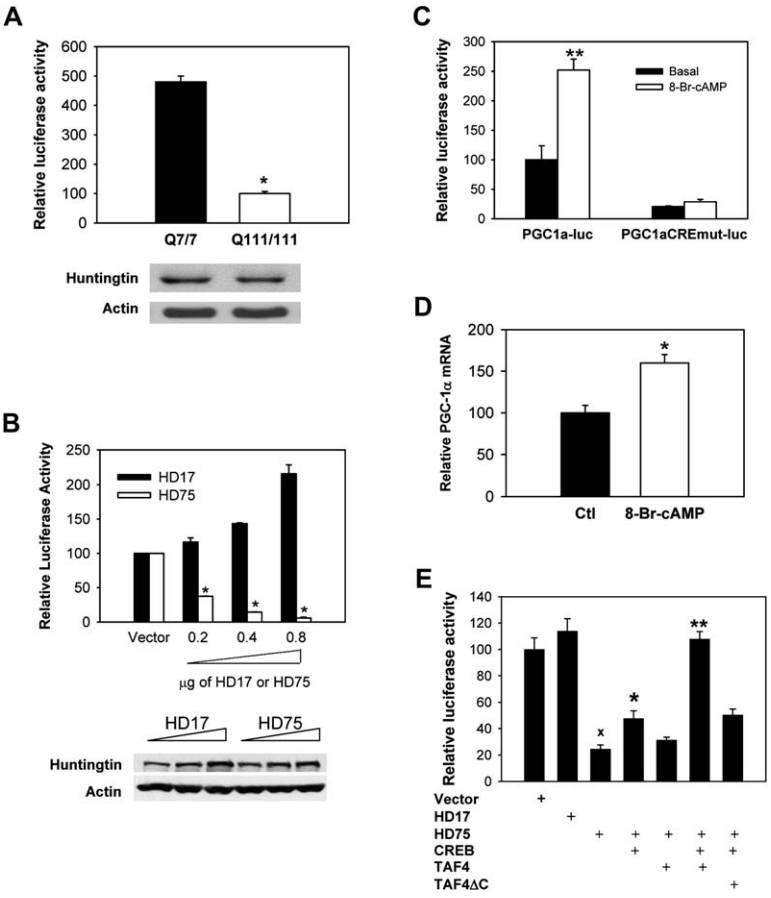

Figure 2. PGC-1α Promoter Activity Is Repressed by Mutant Huntingtin in Striatal Cells

(A) *STHdh*^{Q7} (Q7/7) and *STHdh*^{Q111} (Q111/111) cells were transfected with a luciferase reporter (PGC-1α-luc) encompassing the promoter region −2533 to +78 of mouse PGC-1α gene. Relative reporter activities were normalized to the activity of the promoter-less luciferase reporter construct, pGL3-Basic. Expression of endogenous huntingtin and β-actin was determined by Western blotting. Graphs represent means ± SEM of three experiments. *p < 0.0001 versus Q7/7.

(B) Striatal *STHdh*^{Q7} cells were transfected with PGC-1α-Luc reporter along with varying amounts (0.2 μg, 0.4 μg, and 0.8 μg) of plasmid expressing full-length wild-type (HD17) or mutant huntingtin (HD75). Expression of mutant huntingtin, but not the wild-type, repressed PGC-1α promoter activity in a dose-dependent manner. Protein expression was verified by Western blotting (shown below the graph). *p < 0.0001 versus vector control.

(C) Cyclic-AMP treatment reversed the inhibition of PGC-1α promoter activity in mutant *STHdh*^{Q111} striatal cells. *STHdh*^{Q111}cells were transfected with PGC 1α-luc as described in (A) or PGC-1αCREmut-luc with the mutated CRE site. Twenty-four hours after transfection, the cells were treated with 0.5 mM 8-Bromo-cAMP (8-Br-cAMP) and reporter activities measured 24 hr later. Data were normalized to β-galactosidase activity. The relative luciferase activity in cells transfected with the wild-type PGC-1α-luc is arbitrarily shown as 100 ± SEM. Graphs show means ± SEM of at least three independent experiments. **p < 0.001 versus basal (black bar).

(D) Cyclic-AMP treatment induced endogenous PGC-1α mRNA expression in mutant striatal cells. *STHdh*^{Q111}cells were treated with 0.5 mM 8-Br-cAMP for 16 hr and PGC-1α mRNA levels analyzed by real-time PCR. β-actin mRNA was used for normalization. Graphs show means ± SEM of three independent experiments. *p < 0.01 versus untreated control (Ctl).

(E) Mutant huntingtin-mediated repression of PGC-1α promoter is prevented by overexpression of CREB and TAF4. Primary striatal neurons were transfected with PGC-1α-luc, along with plasmids expressing full-length normal (HD17) or mutant huntingtin (HD75). Coexpression of constitutively active CREB and TAF4 completely reversed mutant huntingtin (HD75)-induced inhibition of PGC-1α promoter activity, whereas TAF4ΔC that lacks the C-terminal 250 amino acids did not significantly affect PGC-1α promoter activity. The relative reporter activity in cells transfected with vector alone is arbitrarily shown as 100 ± SEM. Graphs show means ± SEM of at least three independent experiments. ^{X}p < 0.001 versus vector, *p < 0.05 versus HD75, and **p < 0.001 versus HD75.

inhibition of PGC-1α promoter activity, indicating that mutant huntingtin affects the CREB/TAF4 transcriptional pathway. TAF4 interacts with other TAFs primarily via its C-terminal domain, suggesting the importance of this domain for the interactions of TAF4 with the TFIID complex (Asahara et al., 2001). To examine whether the effects of CREB and TAF4 on PGC-1α were dependent on intact C-terminal domain of TAF4, we coexpressed the C-terminal deletion mutant of TAF4 in primary striatal neurons. No significant effect of TAF4 on PGC-1α promoter activity was observed when the C terminus of TAF4 was deleted, suggesting that this domain is required to reverse the repression of the PGC-1α promoter by mutant huntingtin (Figure 2E).

Together, these results show that mutant huntingtin inhibits transcription of PGC-1α by interfering with the CREB/TAF4 acting on the PGC-1α promoter.

Mutant Huntingtin Is Associated with PGC-1α Promoter in Striatal Cells and HD Mice

We next used chromatin immunoprecipitation (ChIP) assay to determine occupancy of transcription factors at PGC-1α gene in striatal tissues of wild-type and HD KI mice (Figure 3A), R6/2 HD mice (Figure 3B), and in striatal cells derived from wild-type and HD KI mice (Figure 3C). Unexpectedly, we found mutant huntingtin protein to occupy the PGC-1α promoter region in the brains and cells of HD KI mice (Figures 3A and 3C), while presence of wild-type huntingtin was not detected at this promoter. By contrast, occupancy by CREB and TAF4 at the PGC-1α promoter was not substantially altered in wild-type and HD KI cells.

To investigate whether increased occupancy of PGC-1α promoter by mutant huntingtin results in altered PGC-1α transcription in vivo, RNA polymerase II chromatin immunoprecipitations (RNAPol-ChIP) were performed. This

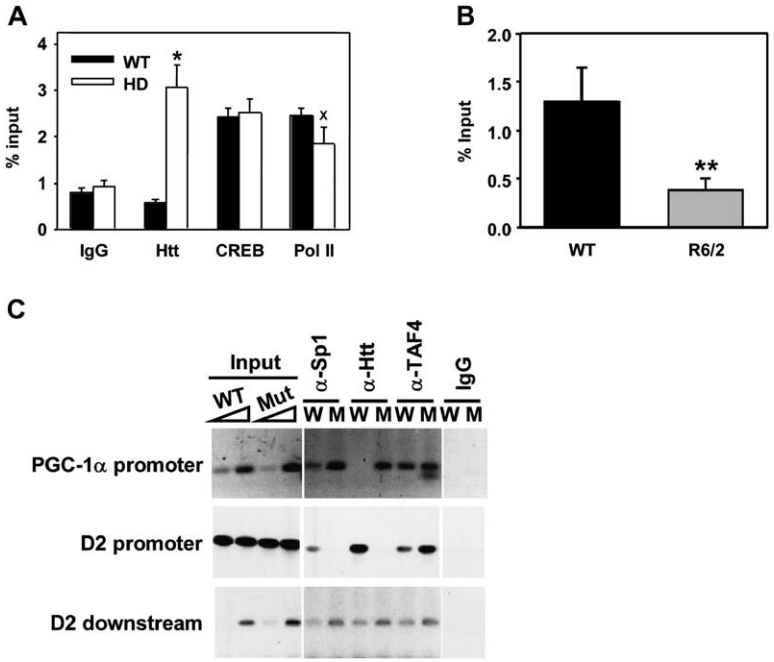

Figure 3. Mutant Huntingtin Occupies PGC-1α Promoter in Mutant Striatal Cells and HD Mice

(A) Brain homogenates of wild-type and HD KI (CAG 140) mice were prepared and ChIP assays of the PGC-1α promoter region performed with indicated antibodies. Presence of mutant huntingtin (Htt), but not wild-type, was detected at the PGC-1α promoter. Graphs show means ± SEM of three independent experiments.*p < 0.0001 versus wild-type, ^{X}p 0.05 versus wild-type.

(B) RNAPol-ChIP assay of the PGC-1α coding region using wild-type and R6/2 mouse brain tissues showed reduced rate of transcription of the PGC-1α gene in vivo. PCR primers correspond to the PGC-1α gene-coding region (+655 to +778) downstream of the transcription start site. Graphs show means ± SEM of three independent experiments. **p < 0.001 versus wild-type.

(C) ChIP analysis of the PGC-1α and dopamine receptor D2 gene promoter in mouse striatal cells expressing wild-type huntingtin (W, *STHdh*$^{Q7/Q7}$) or mutant huntingtin (M, *STHdh*$^{Q111/Q111}$). Formaldehyde cross-linked chromatin was immunoprecipitated with indicated antibodies, and the precipitated material was amplified by PCR using primers specific for each promoter region and stained with ethidium bromide on an agarose gel. A downstream region of the D2 gene was used as a control. Input lanes represent 0.5, 1% (lanes 1, 2) and 0.1, 0.5% (lanes 3, 4) of chromatin.

procedure detects the presence of RNA polymerase II within the coding region of the target gene as a way of measuring active transcription (Sandoval et al., 2004). Using this approach, we found decreased transcription of PGC-1α gene in R6/2 mouse brain as compared to normal littermates (Figure 3B). When genes that are not altered in HD mice, such as albumin, were analyzed by RNAPol-ChIP, no change was observed in polymerase II binding between the normal and HD mice (data not shown).

These results suggest that mutant huntingtin associates with chromatin and interferes with the activation functions of promoter bound transcription factors CREB and TAF4 to repress transcription. Interestingly, we observed occupancy of wild-type huntingtin at a different promoter, the dopamine D2 receptor gene promoter, indicating that wild-type huntingtin may target certain genes to regulate transcription (Figure 3C). These results represent the first evidence that wild-type and mutant huntingtin occupy promoter regions of endogenous neuronal target genes and suggest that differential targeting of huntingtin may help explain specific changes in gene expression observed in HD.

PGC-1α Expression Protects against Mutant Huntingtin-Induced Mitochondrial Dysfunction and Striatal Toxicity

Since PGC-1α regulates mitochondrial respiration (Puigserver and Spiegelman, 2003), decreased levels of PGC-1α may contribute to mitochondrial dysfunction that is characteristic of striatal HD cells (Gines et al., 2003). We therefore directly assessed mitochondrial energy metabolism in wild-type and mutant *STHdh*^{Q111} cells using the MTS assay. This method is based on the reduction of the soluble tetrazolium salt to insoluble formazan product by mitochondrial succinic dehydrogenase. The results revealed that formazan production was significantly reduced by approximately 35% in mutant cells compared with wild-type cells (Figure 4A). Importantly, recombinant adenovirus-mediated expression of PGC-1α in *STHdh*^{Q111} cells significantly reversed the mitochondrial defect as determined by MTS assay, suggesting that upregulation of PGC-1α can rescue the effect of mutant huntingtin on mitochondrial function.

We next analyzed primary striatal cultures that recapitulate features of the neurodegenerative process that occurs in HD. Transfection of full-length mutant huntingtin (HD75) induced neuronal cell death, whereas the wild-type huntingtin did not show any toxic effects, as previously reported (Figure 4B) (Saudou et al., 1998; Dunah et al., 2002). However, when mutant huntingtin is coexpressed in striatal neurons together with PGC-1α, the toxicity of mutant huntingtin was significantly abrogated (Figure 4B), suggesting that expression of PGC-1α in striatal neurons substantially rescues the deleterious effects of mutant huntingtin.

Since our data showed that CREB and TAF4 were able to completely reverse the repressive effects of mutant huntingtin on PGC-1α promoter activity (Figure 2E), we tested whether striatal neurons could be protected against mutant huntingtin by transfecting constitutively

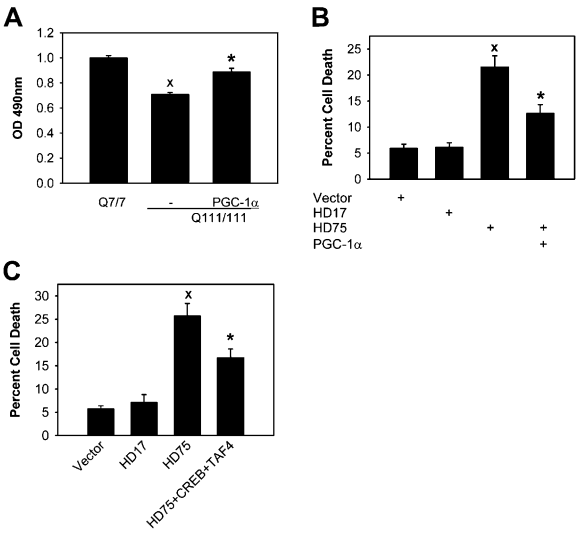

Figure 4. Overexpression of PGC-1α Protects against Mutant Huntingtin-Induced Mitochondrial Dysfunction and Striatal Toxicity

(A) Overexpression of PGC-1α partially rescued the decreased mitochondrial metabolic activity in mutant *STHdh*^{Q111}cells (Q111/111) as measured by MTS assay. Infection of Q111/111 cells with recombinant adenovirus-expressing PGC-1α led to significant upregulation of MTS activity. Expression of PGC-1α was verified by Western blotting and by real-time PCR. Reduction of MTS by cells was measured as units of absorbance at optical density 490 nm. Graphs show means ± SEM of at least three independent experiments. $^{X}p < 0.01$ versus Q7/7 cells. (*STHdh*^{Q7}). *p < 0.01 versus Q111/111 transfected with control adenovirus.

(B) Overexpression of PGC-1α protected against mutant huntingtin-induced striatal toxicity. Primary striatal cultures were transfected with PGC-1α along with full-length mutant HD75 or wild-type HD17 huntingtin. Mutant huntingtin-induced cell death was significantly prevented by the overexpression of PGC-1α. Expression levels of transfected constructs were verified by quantitative immunocytochemistry. Cell nuclei were stained with Hoechst 33258 and condensed and/or fragmented nuclei scored as apoptotic using confocal microscope. Graphs represent means ± SEM of three independent experiments. $^{X}p < 0.001$ compared to HD17 and *p < 0.001 versus HD75.

(C) CREB and TAF4 together protect against mutant huntingtin-induced striatal toxicity. Primary striatal cultures were transfected and analyzed as in (B). Mutant huntingin-induced cell death was significantly prevented by overexpression of the constitutively active CREB and TAF4. Graphs represent means ± SEM of three independent experiments. $^{X}p < 0.001$ compared to HD17 and *p < 0.001 versus HD75.

active CREB along with TAF4. We found that coexpression of CREB and TAF4 resulted in statistically significant protection of striatal cells from the effects of mutant huntingtin (Figure 4C). Coexpression of CREB with TAF4 lacking its C-terminal domain failed to block huntingtin-induced cell death (data not shown), suggesting that intact interactions of TAF4 with TFIID and other factors are required for its protective function. Together, these data demonstrate that CREB/TAF4-dependent regulation of PGC-1α gene, at least in part, mediates the protective effects of PGC-1α in striatal neurons.

Lentiviral-Mediated Delivery of PGC-1α in the Striatum Provides Neuroprotection in the Transgenic Mouse Model of HD

To further test our hypothesis that PGC-1α may be protective in HD, lentiviral vector expressing PGC-1α was directly administered into the striatum of R6/2 transgenic HD mice. We chose to analyze the R6/2 model because it has a well-characterized progressive phenotype that recapitulates many of the neuropathological features observed in HD patients, such as striatal atrophy, cellular atrophy, and huntingtin-positive aggregates (Ferrante et al., 2000).

The striata of 5.5 week-old R6/2 mice were injected with lentiviral vector expressing PGC-1α (Figures 5A and 5B). Using unbiased stereological methods, neuronal volumes were examined 3.5 weeks after the injection. When analyzing a series of sections spanning the injected region of striatum, a statistically significant increase in the mean neuronal volume by 27.8% was observed in striata injected with PGC-1α as compared to contralateral striata that were not injected. No significant change in cell volume was observed in neurons injected with control lentiviral vector expressing green fluorescent protein (GFP) (Figures 5C and 5D). Previous studies have demonstrated that R6/2 mice exhibit progressive atrophy of striatal neurons from about 3 to 12 weeks of age with almost 40% overall decrease in area measurements. In addition, at the age of 9 weeks, when our analysis was performed, volumes of striatal neurons in R6/2 mice decreased by about 30% compared to littermate transgene-negative mice (Figure 5D, Ferrante et al., 2000). Such atrophy of striatal neurons represents a neuropathological feature in R6/2 mice that most closely resembles neuropathology observed in human HD. Here we show that administration of PGC-1α to R6/2 mice completely prevents neuronal atrophy in R6/2 mice. Moreover, the findings in HD mice are in agreement with our studies in cell culture showing that overexpression of PGC-1α protects striatal neurons from toxicity by mutant huntingtin.

Crossbreeding of HD KI Mice with PGC-1α KO Mice Results in Behavioral and Striatal Abnormalities in the HD Mice

The experiments described above demonstrated that expression of PGC-1α is neuroprotective in HD mice. We next examined whether further downregulation of PGC-1α leads to worsening of behavioral and neuropathological abnormalities in HD KI mice that have 140 CAG repeats inserted in the murine huntingtin gene. The 140 CAG KI mice display very mild behavioral and neuropathological abnormalities at baseline (Menalled et al., 2003). When the KI mice were crossbred with PGC-1α KO mice (KI/KO), a significant worsening of motor performance was observed in the 6 month-old crossed mice as compared to the KI or KO littermates (Figure 6A). To investigate whether these behavioral abnormalities in the KI/KO crossed mice were due to alterations in neuronal pathology, we performed a neuropathological evaluation of serial brain sections. Using a silver-staining technique that detects degenerating neurons, we identified early

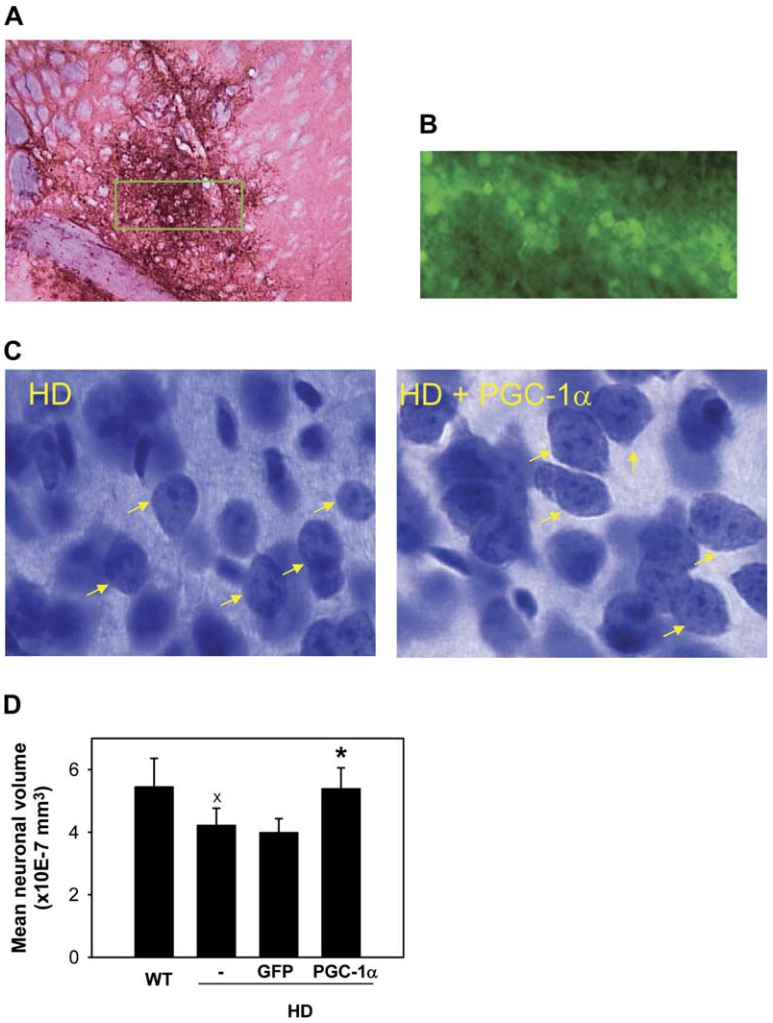

Figure 5. Lentiviral Delivery of PGC-1α in the Striatum of R6/2 Transgenic HD Mice Completely Prevents Atrophy of Striatal Neurons

(A) Expression of lentiviral vectors in the striatum of R6/2 mice 3 weeks after injection. The highest density of the transduced cells was around the injection site (box). Approximately 10% of the striatum showed high expression of lentiviral vectors encoding PGC-1α and GFP as determined by staining with antibodies against His-tag or GFP.

(B) Striatal sections immunostained with antibody recognizing the His-tag of lenti-PGC-1α (green). More than 90% transduced cells displayed neuronal morphology.

(C) Representative striatal sections stained with cresyl violet showing neuronal atrophy (arrows) in noninjected R6/2 striatum (HD) relative to the contralateral side injected with lenti-PGC-1α (HD+PGC-1α).

(D) Neuronal volumes were decreased by 29.2% in 9 week-old R6/2 striata compared to controls (WT). Expression of lenti-PGC-1α in R6/2 striata (HD+PGC-1α) led to increased neuronal volumes by 27.8% compared to noninjected R6/2 neurons (HD) and 35.1% compared to R6/2 neurons injected with lenti-GFP. The striata of R6/2 mice were injected with viral constructs at 5.5 weeks and neuronal volumes analyzed at 9 weeks of age using unbiased stereological methods (MicroBrightField). Average sum of 795 transduced neurons was examined per animal. Y axis shows mean neuronal volumes 5.44 ± 0.717 (WT), 4.21 ± 0.552 (HD), 3.98 ± 0.456 (HD+GFP), and 5.38 ± 0.679 (HD+PGC-1α) × 10^{-7} mm^3. Graphs represent means ± SEM of at least five animals per group. $^{X}p < 0.01$ compared to wild-type and $^{*}p < 0.01$ compared to HD.

neurodegenerative changes in the medial septal nucleus and striatum of the 3 month-old KI/KO crossed mice (Figure 6B). Moreover, a significant reduction in striatal neuronal volumes was observed in the 6 month-old KI/KO mice compared to littermate KI mice (Figure 6C). These results further demonstrate that downregulation of PGC-1α contributes to accelerated degeneration of striatal neurons in HD.

We next examined whether decreased expression of PGC-1α rendered the crossed mice more susceptible to neurotoxin 3-nitropropionic acid (3-NP) known to induce HD-like symptoms. 3-NP is a complex II inhibitor that selectively induces striatal lesions when administered systemically in humans, primates, and rodents. The distribution and pathology of the 3-NP-induced striatal lesions closely resemble those seen in HD (Browne and Beal, 2004). We injected 3-NP directly into the striata of the crossed KI/KO and KI HD mice. Administration of 3-NP produced significantly larger striatal lesions and increased number of degenerating neurons in the KI/KO mice compared to the KI mice (Figure 6D). These results further support the importance of PGC-1α in protection of striatal neurons from metabolic stress and neurodegeneration in HD.

DISCUSSION

Abnormalities in striatal energy metabolism in HD represent an important part of the early pathogenesis of this disease (Koroshetz et al., 1997; Browne and Beal, 2004). For example, decreased striatal metabolism occurs in presymptomatic HD patients, years before the onset of clinical symptoms, indicating that striatal neurons are particularly vulnerable to disruptions of mitochondrial function (Browne and Beal, 2004). This conclusion is underscored by the fact that the PGC-1α KO mice show most striking lesions in the striatum despite the uniform absence in PGC-1α expression in all brain regions (Lin et al., 2004; Leone et al., 2005). We found decreased expression of a number of mitochondrial genes in striata of the PGC-1α KO mice, suggesting that alterations in mitochondrial function may be responsible for the observed

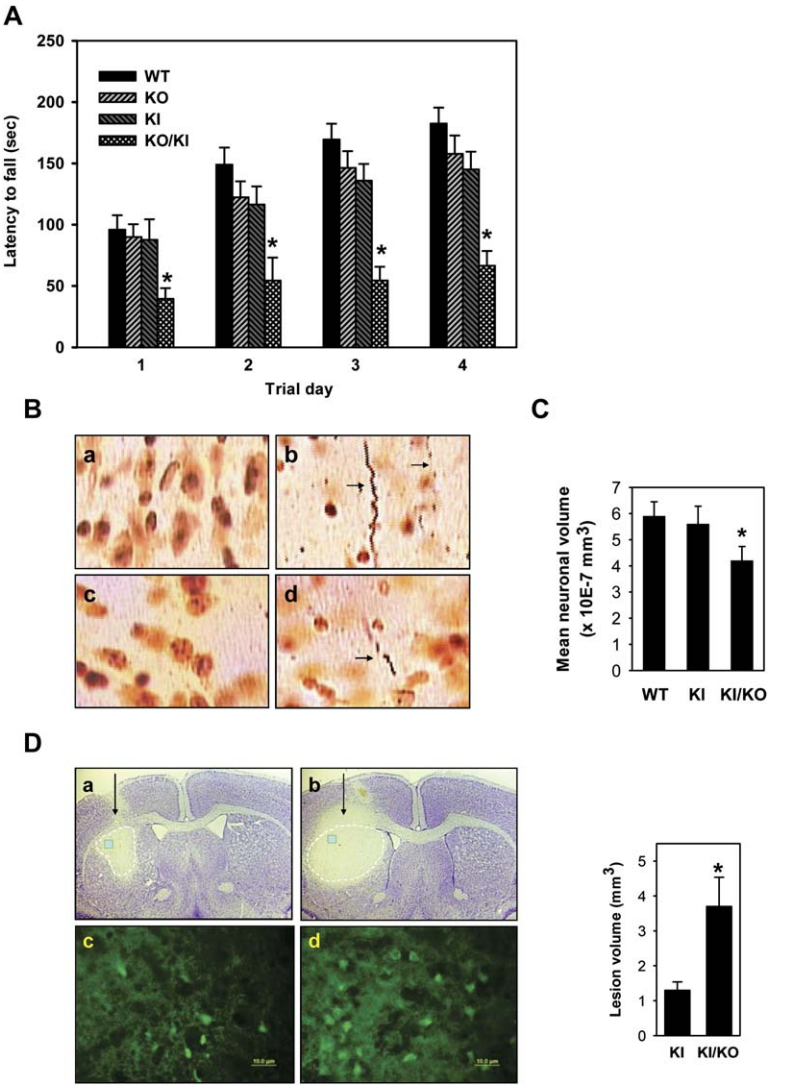

Figure 6. Crossbreeding of HD KI Mice (KI) with PGC-1α KO Mice (KO) Leads to Behavioral Abnormalities and Increased Neurodegeneration in the Crossed Mice (KI/KO)

(A) Rotarod performance is severely impaired in KI/KO mice ($HD^{(CAG)140+/-}$/PGC-$1\alpha^{+/-}$). Wild-type (WT), $HD^{(CAG)140+/-}$ (KI), PGC-$1\alpha^{+/-}$ (KO), and KI/KO mice were tested for performance in four trials per day for 4 consecutive days (n = 20 per group). Bars represent means ± SEM latencies to fall. *p = 0.005 versus KI mice.

(B) Early neuronal degeneration appears in the striatum and septum of KI/KO mice. Brain sections from 3 month-old KI (a and c) and KI/KO (b and d) mice were silver stained to detect disintegrative neuronal processes (arrows) from degenerating neurons in medial septal nucleus (b) and striatum (d) of the KI/KO mice. No degeneration was observed in the septum (a), striatum (c), or any other brain region in the KI mice.

(C) Striatal neuronal volumes were significantly decreased in 6 month-old KI/KO mice. Neuronal volumes were analyzed as described in Figure 5D. Graphs represent means ± SEM volumes from at least five animals in each group. *p < 0.01 compared with KI.

(D) Loss of PGC-1α gene leads to increased susceptibility of HD mice to 3-nitropropionic acid (3-NP). Striata of the KI (a and c) and KI/KO (b and d) mice were injected with 3-NP (75 nmol) and analyzed 24 hr later by Nissl (a and b) and Fluorojade C staining (c and d). Administration of 3-NP resulted in increased size of the lesions (compare a and b) and the number of degenerating neurons (compare c and d) in the KI/KO mice as compared with the KI mice. Stereological analysis of the lesion showed significantly increased volumes in the KI/KO compared to KI mice (n = 8 in each group). Bars represent means ± SEM striatal lesion volume. *p< 0.005 versus KI.

neuropathology in these mice. Although the neuropathologic changes observed in the PGC-1α KO mice appear nonspecific compared to those found in HD, it is striking that the KO mice show such prominent abnormalities in the striatum, the region most affected in HD.

In this study we demonstrate that PGC-1α expression is selectively and significantly downregulated in HD striatal cells and tissues. Our results suggest that a possible mechanism for the observed downregulation of PGC-1α involves transcriptional repression of PGC-1α promoter by mutant huntingtin. We find that mutant huntingtin represses CRE-mediated transcription of PGC-1α by interfering with the CREB/TAF4 transcriptional pathway in striatal neurons. Interestingly, ChIP analysis revealed that mutant but not wild-type huntingtin was found associated with the endogenous PGC-1α promoter, suggesting that the mutant protein disrupts the function of promoter bound transcription factors. Reduced CRE-dependent transcription has been previously observed as an early abnormality in HD pathogenesis, but the target genes of the CRE-dependent transcription in HD have not been determined (Gines et al., 2003; Sugars and Rubinsztein, 2003). Moreover, ablation of CREB and CREM in the postnatal CNS produces a progressive neurodegeneration in striatum that is reminiscent of HD, suggesting that CREB may play an important role in HD pathogenesis (Mantamadiotis et al., 2002). Mutant huntingtin has been shown previously to directly repress transcription of Sp1-driven genes by uncoupling the interactions of activator (Sp1) with the coactivator TAF4 (Dunah et al., 2002). Since both Sp1 and CREB interact with TAF4, we think these interactions are directly targeted by mutant huntingtin in certain promoter context. We found that huntingtin interacts with both the glutamine-rich central domain and the C-terminal domain of TAF4 and that the C-terminal domain is required for protection against huntingtin-induced transcriptional dysregulation and neuronal cell death (Figure 2E, Dunah et al., 2002). The conserved

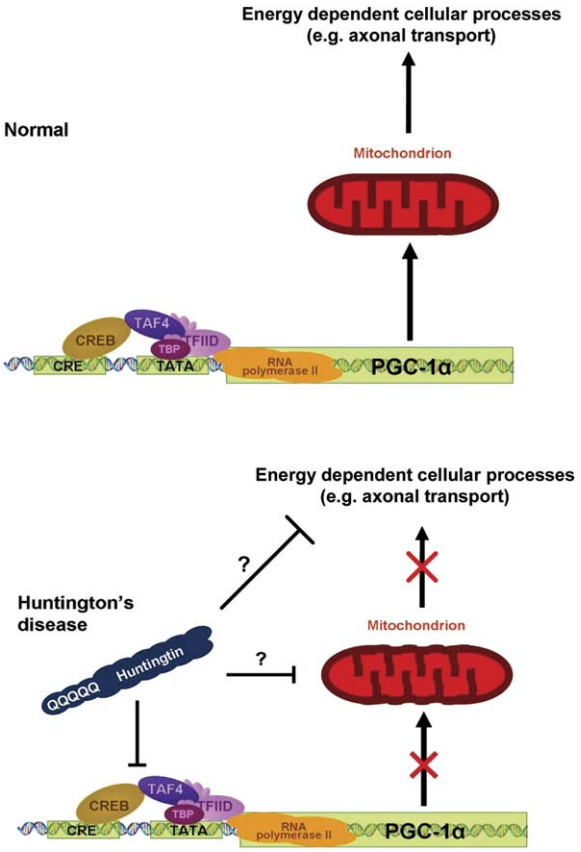

Figure 7. Model for Regulation of PGC-1α in Huntington's Disease (HD)

In a normal state, PGC-1α regulates metabolic programs and maintains energy homeostasis in the CNS (upper panel). In HD, mutant huntingtin interferes with CREB and TAF4 regulation of PGC-1α transcription that leads to inhibited expression of PGC-1α. Inhibition of PGC-1α expression limits the ability of the vulnerable neurons to adequately respond to energy demands in HD (lower panel). Direct toxic effects of mutant huntingtin on mitochondria and other energy-dependent neuronal processes such as axonal transport may worsen when protective function of PGC-1α is inhibited.

C-terminal domain of TAF4 participates in a number of protein-protein interactions, including several TAFs in the TFIID complex (Furukawa and Tanese, 2000; Asahara et al., 2001). These findings and the recent report that atrophin, which causes another polyglutamine disease (DRPLA), also binds to the C-terminal domain of TAF4 (Shimohata et al., 2000), suggest that TAF4, probably in the context of TFIID, represents a key target of polyglutamine proteins such as huntingtin.

Interestingly, we find that PGC-1α levels were decreased in MSN but upregulated in nNOS interneurons isolated from HD mice. It is well established that striatal MSN selectively degenerate whereas nNOS interneurons survive in HD (Ferrante et al., 1985). Previous studies showed that mutant huntingtin accumulates in the nucleus of MSN but not in nNOS interneurons (Wheeler et al., 2000). Since our ChIP data suggest that inhibition of PGC-1α transcription in HD involves recruitment of mutant huntingtin to PGC-1α promoter, we think that the absence of mutant huntingtin in the nucleus of interneurons may partly explain increased levels of PGC-1α mRNA in these cells.

Here, a model is proposed where mutant huntingtin affects mitochondrial function by interfering with PGC-1α gene transcription (Figure 7). We hypothesize that in the normal state, PGC-1α regulates metabolic programs and maintains energy homeostasis in the CNS, whereas inhibition of PGC-1α transcription by mutant huntingtin leads to defects in energy metabolism and dysfunction of neurons that are most vulnerable to metabolic stress, such as striatal neurons. Our results indicate that inhibition of PGC-1α function by mutant huntingtin limits the ability of striatal neurons to adequately respond to metabolic demands in HD. Such disruption in energy homeostasis in HD may lead to alteration of multiple cellular functions and ultimately results in neurodegeneration. In addition, mutant huntingtin directly targets cellular processes with high energy requirements such as axonal transport (Gunawardena et al., 2003; Szebenyi et al., 2003; Gauthier et al., 2004). Moreover, expanded polyglutamines alter mitochondrial membrane depolarization, making cells more vulnerable to metabolic stress (Panov et al., 2002; Brustovetsky et al., 2003; Choo et al., 2004). Such direct toxic effects of mutant huntingtin may become more pronounced when the protective function of PGC-1α is inhibited (Figure 7). It will be of interest to determine whether stimulation of the pathways of energy metabolism controlled by PGC-1α could provide potential clinical benefit at an early stage of HD.

EXPERIMENTAL PROCEDURES

Striatal Cell Lines and Primary Striatal Neurons

Immortalized wild-type *STHdh*$^{Q7/Q7}$ striatal neuronal progenitor cells expressing endogenous normal huntingtin and homozygous mutant *STHdh*$^{Q111/Q111}$ lines expressing endogenous mutant huntingtin with 111 glutamines were cultured as described (Gines et al., 2003). Recombinant adenoviral vector containing FLAG-tagged PGC-1α (Ad-Flag-PGC-1α) and PGC-1α-luc were generously provided by Bruce Spiegelman lab. Primary striatal neurons were cultured from E18 Sprague-Dawley rats as described (Dunah et al., 2002). For measurements of neuronal cell death, neurons were scored as apoptotic if they had pyknotic or fragmented nuclei. Cells were transfected using Lipofectamine 2000 (Invitrogen) as described (Dunah et al., 2002). The PGC-1α promoter-luciferase reporter was described previously (Handschin et al., 2003). Luciferase activity was determined 48 hr after transfection using the luciferase assay kit (Promega) and normalized to β-galactosidase activity (Clontech). The relative activity was normalized to the activity of the promoter-less reporter, pGL3-Basic (Promega). The metabolic activity of mitochondria was assayed by using a modified MTS assay kit (Promega).

Quantitative Real-Time PCR and Immunoblot Analysis

Total RNA was isolated from cultured cells or brain tissues using RNeasy Lipid Tissue kit (Qiagen). Postmortem human brain tissues were from asymptomatic carriers of HD mutation (CAG 45-57, Grade 0) and age- and gender-matched normal controls with similar postmortem interval. R6/2 transgenic HD mice were obtained from Jackson Laboratory. RNA was analyzed by quantitative real-time PCR using SYBR Green (Applied Biosystems). Primer sequences used in all

PCR experiments are listed in Table S1. Western blots were performed as described (Dunah et al., 2002). The blots were probed with the following primary antibodies: PGC-1α (K-15) (sc-5816, Santa Cruz Biotechnology), Oxphos Complex IV subunit I (1D6, BD Biosciences Pharmingen) Cytochrome C (7H8.2C12, Chemicon), actin (sc-1616, Santa Cruz).

Gene-Expression Profiling

Total RNA was extracted from striata of PGC-1α KO mice and littermate controls and analyzed by RNA 6000 Nano LabChip kit on a 2100 Bioanalyzer (Agilent Technologies) to ensure integrity of RNA. The RNA was processed according to the standard Affymetrix protocol and analyzed using the Mouse Genome 430 2.0 Gene Chips. The functional correlation of gene sets systemically altered in expression profiles of PGC-1α KO mice and a previously published human HD expression (Hodges et al., 2006) was assessed using Gene Set Enrichment Analysis (Subramanian et al., 2005).

ChIP Assay

Homogenized brain tissues were forced through a 70 μm cell-strainer cap followed by incubation in Dulbecco's modified Eagle medium containing 1% formaldehyde. The samples were sonicated with a Fisher sonicator for 12 × 15 s cycles at 60% output power, the lysates centrifuged at 13,000 × g for 10 min, and diluted 10-fold in ChIP dilution buffer. ChIP assay was performed following published procedures (Takahashi et al, 2000). RNAPol-ChIP was carried out as described (Sandoval et al., 2004). Primer sequences are listed in Table S1.

Crossbreeding and Analysis of HD Mice

PGC-1α KO mice (Leone et al. 2005) were crossed with HD KI mice (Menalled et al., 2003) to obtain all possible viable genotypes, as determined by PCR with tail-tip DNA and sequencing to confirm genotype and CAG repeat length. Recombinant lentiviral vectors expressing PGC-1α were generated as described (Sena-Esteves et al. 2004) and stereotaxically injected into the striatum of 5.5 week-old R6/2 mice. After 3.5 weeks serial brain sections were examined stereologically as described (Ferrante et al., 2000). Briefly, unbiased estimates of number–weighted mean neuronal volumes were determined using the optical fractionator and nucleator probes (Micro BrightField; Williston, VT). Objective used to estimate the volumes of striatal cells was ×63; counting frame 50 × 50 μm, sampling grid 100 × 100 (x and y); average section thickness after histological processing, 7.0 μm (top guard zone, 3μm, and bottom, 4μm); average sum of neurons analyzed per animal, 795. ANOVA with post hoc t tests was performed to identify significant differences. Silver staining of sections was performed as described in the FD Neurosilver kit (FD Neurotechnologies,). Fluoro-Jade C staining was performed according to the supplier's manual (HistoChem). Motor performance was performed using the rotarod apparatus (Economex Rotarod, Columbus Instruments). The mice were pretrained on the rotarod for five trials at low speed for up to 120 sec and tested for four trials per day for 4 consecutive days. Rotating rod underwent a linear acceleration from 4 to 40 rpm over the first 6 min of the trial and then remained at maximum speed for the remaining 4 min. For the 3-NP experiments, a total of 75 nmol of 3-NP in a volume of 1 μl was injected into striatum at a rate of 0.2 μl/min. All animals were sacrificed 24 hr after 3-NP injections and brains postfixed in PLP fixative for 16 hr and then immersed in 25% sucrose in 0.1 M PB, pH 7.4 for 48 hr. Laser capture microdissection was performed as described (Zucker et al. 2005). Briefly, coronal 8 μm striatal sections from four CAG140 KI and four wild-type mice were cut on a cryostat and thaw-mounted on non-coated glass slides. For visualization of MSN or nNOS positive interneurons, sections were stained with methylene blue or rabbit anti-nNOS antibody (N7155, Sigma), respectively. At least 1000 striatal neurons per group were dissected using the PixCell II LCM instrument and total RNA isolated by PicoPure RNA kit (Arcturus).

Supplemental Data

Supplemental Data include one figure, one table, and experimental procedures and can be found with this article online at http://www.cell.com/cgi/content/full/127/1/59/DC1/.

ACKNOWLEDGMENTS

We thank Hongwei Jin for help with stereotaxic surgery; Geoff Greene from MicroBrightField, Inc. and Jonathan H. Fox for help with stereology experiments; Daniel P. Kelly and Teresa C. Leone for PGC-1α KO mice and helpful discussions; Fu Du for help with silver staining; and Jiandie Lin, Bruce Spiegelman, Anne B. Young, Tong Lin, Katrin Lindenberg, Robert Ferrante, Birgit Zucker, and Nicole Deglon for helpful discussions or comments on the manuscript. We thank Marcy MacDonald for striatal cell lines and Harvard Brain Tissue Resource Center, Jean-Paul Vonsattel, and Kathy Newell for human postmortem brain tissues. This work was supported by R01NS050352 and P01NS045242 (D.K.). F.B. was supported by Fulbright Fellowship.

Received: June 1, 2006
Revised: August 15, 2006
Accepted: September 8, 2006
Published: October 5, 2006

REFERENCES

Alba, M.M., and Guigo, R. (2004). Comparative analysis of amino acid repeats in rodents and humans. Genome Res. *14*, 549–554.

Antonini, A., Leenders, K.L., Spiegel, R., Meier, D., Vontobel, P., Weigell-Weber, M., Sanchez-Pernaute, R., de Yebenez, J.G., Boesiger, P., Weindl, A., and Maguire, R.P. (1996). Striatal glucose metabolism and dopamine D2 receptor binding in asymptomatic gene carriers and patients with Huntington's disease. Brain *11*, 2085–2095.

Asahara, H., Santoso, B., Guzman, E., Du, K., Cole, P.A., Davidson, I., and Montminy, M. (2001). Chromatin-dependent cooperativity between constitutive and inducible activation domains in CREB. Mol. Cell. Biol. *21*, 7892–7900.

Browne, S.E., and Beal, M.F. (2004). The energetics of Huntington's disease. Neurochem. Res. *29*, 531–546.

Brustovetsky, N., Brustovetsky, T., Purl, K.J., Capano, M., Crompton, M., and Dubinsky, J.M. (2003). Increased susceptibility of striatal mitochondria to calcium-induced permeability transition. J. Neurosci. *23*, 4858–4867.

Choo, Y.S., Johnson, G.V., MacDonald, M., Detloff, P.J., and Lesort, M. (2004). Mutant huntingtin directly increases susceptibility of mitochondria to the calcium-induced permeability transition and cytochrome c release. Hum. Mol. Genet. *13*, 1407–1420.

Du, K., Asahara, H., Jhala, U.S., Wagner, B.L., and Montminy, M. (2000). Characterization of a CREB gain-of-function mutant with constitutive transcriptional activity in vivo. Mol. Cell. Biol. *20*, 4320–4327.

Dunah, A.W., Jeong, H., Griffin, A., Kim, Y.M., Standaert, D.G., Hersch, S.M., Mouradian, M.M., Young, A.B., Tanese, N., and Krainc, D. (2002). Sp1 and TAFII130 transcriptional activity disrupted in early Huntington's disease. Science *296*, 2238–2243.

Ferrante, R.J., Kowall, N.W., Beal, M.F., Richardson, E.P., Jr., Bird, E.D., and Martin, J.B. (1985). Selective sparing of a class of striatal neurons in Huntington's disease. Science *230*, 561–563.

Ferrante, R.J., Andreassen, O.A., Jenkins, B.G., Dedeoglu, A., Kuemmerle, S., Kubilus, J.K., Kaddurah-Daouk, R., Hersch, S.M., and Beal, M.F. (2000). Neuroprotective effects of creatine in a transgenic mouse model of Huntington's disease. J. Neurosci. *20*, 4389–4397.

Finck, B.N., and Kelly, D.P. (2006). PGC-1 coactivators: inducible regulators of energy metabolism in health and disease. J. Clin. Invest. *116*, 615–622.

Furukawa, T., and Tanese, N. (2000). Assembly of partial TFIID complexes in mammalian cells reveals distinct activities associated with individual TATA box-binding protein-associated factors. J. Biol. Chem. *275*, 29847–29856.

Gauthier, L.R., Charrin, B.C., Borrell-Pages, M., Dompierre, J.P., Rangone, H., Cordelieres, F.P., De Mey, J., MacDonald, M.E., Lessmann, V., Humbert, S., and Saudou, F. (2004). Huntingtin controls neurotrophic support and survival of neurons by enhancing BDNF vesicular transport along microtubules. Cell *118*, 127–138.

Gines, S., Seong, I.S., Fossale, E., Ivanova, E., Trettel, F., Gusella, J.F., Wheeler, V.C., Persichetti, F., and MacDonald, M.E. (2003). Specific progressive cAMP reduction implicates energy deficit in presymptomatic Huntington's disease knock-in mice. Hum. Mol. Genet. *12*, 497–508.

Grafton, S.T., Mazziotta, J.C., Pahl, J.J., St George-Hyslop, P., Haines, J.L., Gusella, J., Hoffman, J.M., Baxter, L.R., and Phelps, M.E. (1992). Serial changes of cerebral glucose metabolism and caudate size in persons at risk for Huntington's disease. Arch. Neurol. *49*, 1161–1167.

Gunawardena, S., Her, L.S., Brusch, R.G., Laymon, R.A., Niesman, I.R., Gordesky-Gold, B., Sintasath, L., Bonini, N.M., and Goldstein, L.S. (2003). Disruption of axonal transport by loss of huntingtin or expression of pathogenic polyQ proteins in *Drosophila*. Neuron *40*, 25–40.

Handschin, C., Rhee, J., Lin, J., Tarr, P.T., and Spiegelman, B.M. (2003). An autoregulatory loop controls peroxisome proliferator-activated receptor gamma coactivator 1alpha expression in muscle. Proc. Natl. Acad. Sci. USA *100*, 7111–7116.

Herzig, S., Long, F., Jhala, U.S., Hedrick, S., Quinn, R., Bauer, A., Rudolph, D., Schutz, G., Yoon, C., Puigserver, P., et al. (2001). CREB regulates hepatic gluconeogenesis through the coactivator PGC-1. Nature *413*, 179–183.

Hodges, A., Strand, A.D., Aragaki, A.K., Kuhn, A., Sengstag, T., Hughes, G., Elliston, L.A., Hartog, C., Goldstein, D.R., Thu, D., et al. (2006). Regional and cellular gene expression changes in human Huntington's disease brain. Hum. Mol. Genet. *15*, 965–977.

Koroshetz, W.J., Jenkins, B.G., Rosen, B.R., and Beal, M.F. (1997). Energy metabolism defects in Huntington's disease and effects of coenzyme Q10. Ann. Neurol. *41*, 160–165.

Kuwert, T., Lange, H.W., Boecker, H., Titz, H., Herzog, H., Aulich, A., Wang, B.C., Nayak, U., and Feinendegen, L.E. (1993). Striatal glucose consumption in chorea-free subjects at risk of Huntington's disease. J. Neurol. *241*, 31–36.

Leone, T.C., Lehman, J.J., Finck, B.N., Schaeffer, P.J., Wende, A.R., Boudina, S., Courtois, M., Wozniak, D.F., Sambandam, N., Bernal-Mizrachi, C., et al. (2005). PGC-1alpha deficiency causes multi-system energy metabolic derangements: muscle dysfunction, abnormal weight control and hepatic steatosis. PLoS Biol. *3*, e101.

Lin, J., Wu, P., Tarr, P., St-Pierre, J., Zhang, J., Mootha, V.K., Jager, S., Vianna, C., Reznick, R., Manieri, M., et al. (2004). Defects in adaptive energy metabolism with hyperactivity in PGC-1alpha mutant mice. Cell *119*, 121–135.

Mantamadiotis, T., Lemberger, T., Bleckmann, S.C., Kern, H., Kretz, O., Martin Villalba, A., Tronche, F., Kellendonk, C., Gau, D., Kapfhammer, J., et al. (2002). Disruption of CREB function in brain leads to neurodegeneration. Nat. Genet. *31*, 47–54.

Menalled, L.B., Sison, J.D., Dragatsis, I., Zeitlin, S., and Chesselet, M.F. (2003). Time course of early motor and neuropathological anomalies in a knock-in mouse model of Huntington's disease with 140 CAG repeats. J Comp Neurol. *465*, 11–26.

Panov, A.V., Gutekunst, C.A., Leavitt, B.R., Hayden, M.R., Burke, J.R., Strittmatter, W.J., and Greenamyre, J.T. (2002). Early mitochondrial calcium defects in Huntington's disease are a direct effect of polyglutamines. Nat. Neurosci. *5*, 731–736.

Puigserver, P., and Spiegelman, B.M. (2003). Peroxisome proliferator-activated receptor-gamma coactivator 1 alpha (PGC-1 alpha): transcriptional coactivator and metabolic regulator. Endocr. Rev. *24*, 78–90.

Saluja, D., Vassallo, M.F., and Tanese, N. (1998). Distinct subdomains of human TAFII130 are required for interactions with glutamine-rich transcriptional activators. Mol. Cell. Biol. *18*, 5734–5743.

Sandoval, J., Rodriguez, J.L., Tur, G., Serviddio, G., Pereda, J., Boukaba, A., Sastre, J., Torres, L., Franco, L., and Lopez-Rodas, G. (2004). RNAPol-ChIP: a novel application of chromatin immunoprecipitation to the analysis of real-time gene transcription. Nucleic Acids Res. *32*, 1–8.

Saudou, F., Finkbeiner, S., Devys, D., and Greenberg, M.E. (1998). Huntingtin acts in the nucleus to induce apoptosis but death does not correlate with the formation of intranuclear inclusions. Cell *95*, 55–66.

Shimohata, T., Nakajima, T., Yamada, M., Uchida, C., Onodera, O., Naruse, S., Kimura, T., Koide, R., Nozaki, K., Sano, Y., et al. (2000). Expanded polyglutamine stretches interact with TAFII130, interfering with CREB-dependent transcription. Nat. Genet. *26*, 29–36.

Sena-Esteves, M., Tebbets, J.C., Steffens, S., Crombleholme, T., and Flake, A.W. (2004). Optimized large-scale production of high titer lentivirus vector pseudotypes. J. Virol. Methods *122*, 131–139.

Subramanian, A., Tamayo, P., Mootha, V.K., Mukherjee, S., Ebert, B.L., Gillette, M.A., Paulovich, A., Pomeroy, S.L., Golub, T.R., Lander, E.S., and Mesirov, J.P. (2005). Gene set enrichment analysis: a knowledge-based approach for interpreting genome-wide expression profiles. Proc. Natl. Acad. Sci. USA *102*, 15545–15550.

Sugars, K.L., and Rubinsztein, D.C. (2003). Transcriptional abnormalities in Huntington disease. Trends Genet. *19*, 233–238.

Szebenyi, G., Morfini, G.A., Babcock, A., Gould, M., Selkoe, K., Stenoien, D.L., Young, M., Faber, P.W., MacDonald, M.E., McPhaul, M.J., and Brady, S.T. (2003). Neuropathogenic forms of huntingtin and androgen receptor inhibit fast axonal transport. Neuron *40*, 41–52.

Takahashi, Y., Rayman, J.B., and Dynlacht, B.D. (2000). Analysis of promoter binding by the E2F and pRB families in vivo: distinct E2F proteins mediate activation and repression. Genes Dev. *14*, 804–816.

Trettel, F., Rigamonti, D., Hilditch-Maguire, P., Wheeler, V.C., Sharp, A.H., Persichetti, F., Cattaneo, E., and MacDonald, M.E. (2000). Dominant phenotypes produced by the HD mutation in STHdh(Q111) striatal cells. Hum. Mol. Genet. *9*, 2799–2809.

Vonsattel, J.P., and DiFiglia, M. (1998). Huntington disease. J. Neuropathol. Exp. Neurol. *57*, 369–384.

Wheeler, V.C., White, J.K., Gutekunst, C.A., Vrbanac, V., Weaver, M., Li, X.J., Li, S.H., Yi, H., Vonsattel, J.P., Gusella, J.F., et al. (2000). Long glutamine tracts cause nuclear localization of a novel form of huntingtin in medium spiny striatal neurons in HdhQ92 and HdhQ111 knock-in mice. Hum. Mol. Genet. *9*, 503–513.

Zhai, W., Jeong, H., Cui, L., Krainc, D., and Tjian, R. (2005). In vitro analysis of huntingtin-mediated transcriptional repression reveals multiple transcription factor targets. Cell *123*, 1241–1253.

Zoghbi, H.Y., and Orr, H.T. (2000). Glutamine repeats and neurodegeneration. Annu. Rev. Neurosci. *23*, 217–247.

Zucker, B., Luthi-Carter, R., Kama, J.A., Dunah, A.W., Stern, E.A., Fox, J.H., Standaert, D.G., Young, A.B., and Augood, S.J. (2005). Transcriptional dysregulation in striatal projection- and interneurons in a mouse model of Huntington's disease: neuronal selectivity and potential neuroprotective role of HAP1. Hum. Mol. Genet. *14*, 179–189.